

# **A Parallel-Processing Coupled Wave/Current/Sediment Transport Model**

Dr. David J.S. Welsh and Dr. Keith W. Bedford  
Dept. of Civil and Environmental Engineering and Geodetic Science  
The Ohio State University

Rong Wang and Dr. Ponnuswamy Sadayappan  
Dept. of Computer and Information Science  
The Ohio State University

## **Abstract**

Predictions of water elevations, currents, wave heights, and sediment transport are important inputs in the planning of military activities in the marine environment. This paper documents the coupling of advanced wave, circulation, and sediment transport models using a physically realistic combined bottom boundary layer model, parallel-processing strategies, and high performance computing facilities at the U.S. Army Engineer Research and Development Center. This work is an extension of previous research that coupled circulation and wave models at the air-sea boundary layer. The models used are the WAM wave model, the CH3D-SED circulation and sediment transport model, and the WCBL bottom boundary layer model. The coupled system has been named the COupled MArine Prediction System (COMAPS). The system has been deployed for the Adriatic Sea and results are presented for coupled and non-coupled hindcasts. The simulation speed of COMAPS for different combinations of WAM, CH3D-SED, and WCBL processes is also discussed.

## **Introduction**

The accurate prediction of sediment transport and suspended sediment concentrations are important issues for a number of military activities. These activities include navigation channel maintenance and dredged material disposal, and the prediction of submarine sediment clouds in which vessels and assault troops can elude detection. Both wave and current motions cause sediment transport and suspension, but in traditional models only current-induced effects have been considered. In coastal waters, wave effects become important and their inclusion can greatly improve the accuracy of sediment predictions. Physics representations of combined wave-current bottom boundary layers have been developed in the last two decades (Glenn and Grant, 1987, for example), but due to the performance limitations of sequential computer systems, coupled numerical simulations have been limited to simplified models or idealized wave and current fields.

The aim of this research was to couple advanced marine circulation, sediment transport, wave, and boundary layer models to take full advantage of the U.S. Army Engineer Research and Development Center Major Shared Research Center (ERDC MSRC) high performance computing facilities. A parallel-processing coupled system has been developed using the WAM wind-wave model, the CH3D-SED circulation and sediment transport model, and the WCBL wave-current bottom boundary layer model. This research is an extension of the work documented in Welsh et al. (1999), where the WAM and CH3D models were coupled at the

atmospheric boundary layer. The WAM/CH3D-SED/WCBL modeling system, including both atmospheric and bottom boundary layer couplings, has been named the COupled MArine Prediction System (COMAPS).

## Models used

The WAM wind-wave model (WAMDI, 1988) predicts unsteady frequency-direction spectra of wave energy on a regular, spherical (longitude/latitude) grid. Significant wave heights, mean wave periods, and mean wave directions are calculated from the spectra. WAM cycle 4 (Gunther et al., 1992) is used here. This version is based on the wave action density conservation equation, in terms of frequencies relative to the local current, and includes advanced, “third-generation” physics (Komen et al., 1994) in the calculation of wind input, nonlinear wave-wave interaction, and dissipation source/sink terms.

The CH3D marine circulation model (Chapman et al., 1996) predicts unsteady three-dimensional current, temperature, and salinity fields, and two-dimensional water surface elevation fields. The model solves conservation equations for mass, momentum, thermal energy, and salinity using a curvilinear horizontal grid and a sigma-layer (terrain following) vertical grid.

The SED sediment transport and concentration model predicts three-dimensional fields of sediment concentration for an arbitrary number of user-specified sediment size classes. In CH3D-SED (Spasojevic and Holly, 1994), the SED sediment calculations are fully integrated with the CH3D circulation calculations. The SED model accounts for erosion, deposition, and bedload transport in an active layer at the top of the bed, and also calculates suspended sediment transport. Sediment mass conservation equations are solved for each size class both in the active layer and at each CH3D-SED vertical sigma-layer.

The origins of the WCBL model lie with the wave-current boundary layer theory of Grant and Madsen (1979). This work addressed wave-dominated conditions and did not account for stratification due to suspended sediment. Glenn and Grant (1987) added the stratification effect, and Keen and Glenn (1998) extended the applicability of the theory to a wider range of wave-current regimes. The original WCBL code was written by Lee (1992), with the modifications of Keen and Glenn (1998) added for the COMAPS project.

The WCBL model uses two dimensionless shear velocities that represent the interacting effects of the wave and current boundary layers. The maximum combined shear velocity is given by

$$U_{*cw} = \left( \frac{f_{cw}}{2} U_b^2 \mathbf{a} \right)^{0.5}, \quad (1)$$

where  $U_b$  is the wave-induced orbital velocity at the top of the wave boundary layer,  $\mathbf{a}$  is a dimensionless function that accounts for current effects, and  $f_{cw}$  is a combined wave-current friction factor calculated from a nonlinear, directional function of  $U_b$ , the near-bed current, and parameters describing the sediment size classes. The time-averaged shear velocity is given by

$$U_{*c} = \left( \frac{f_{cw}}{2} U_b^2 V_2 \right)^{0.5}, \quad (2)$$

where  $V_2$  is another dimensionless function, similar to  $\mathbf{a}$ , first used in Grant and Madsen (1979).  $U_{*cw}$  and  $U_{*c}$  correspond to wave-current and current-only effects, respectively, with  $f_{cw}$ ,  $\mathbf{a}$ , and  $V_2$  accounting for the interactions between the boundary layers. It should be noted that (1) and (2) are similar in form to the widely used Taylor drag law.

WCBL uses (1) and (2) in the calculation of the apparent bottom roughness due to the combined boundary layer:

$$k_{bc} = k_b \left( 30 \frac{\mathbf{d}_w}{k_b} \right)^{\left( 1 - \frac{U_{*c}}{U_{*cw}} \right)}, \quad (3)$$

where  $\mathbf{d}_w$ , the height of the wave boundary layer, scales with  $U_{*cw}$ , and  $k_b$  is the physical bottom roughness, which includes contributions due to active layer grain size, ripple height and steepness, and ‘breakoff’ sediment transport in high-shear conditions. For large waves and small currents, function  $V_2 \rightarrow 0$ , while function  $\mathbf{a} \rightarrow 1$ . This means that (3) gives  $k_{bc} \approx 30\mathbf{d}_w$ , which is the roughness for a pure wave boundary layer. Conversely, for small waves and large currents, the ratio  $(V_2/\mathbf{a}) \rightarrow 1$ , and  $k_{bc}$  from (3) reverts to the current boundary layer roughness  $k_b$ .

The current profile for the combined boundary layer is

$$U(z) = \frac{U_{*c}}{\mathbf{k}} \left( \ln \frac{30z}{k_{bc}} \right) + \mathbf{b}\mathbf{a} \ln \frac{z}{\mathbf{d}_w}, \quad (4)$$

where  $\mathbf{b}$  is a constant.

The solution procedure in WCBL has two iterative stages. Unstratified wave-current boundary layer theory is first used to calculate a representative boundary layer current,  $U_a$ . A known current,  $U_r$ , which applies at reference elevation  $Z_r$ , is used as the first guess for  $U_a$ . The convergence criterion is that  $U_r$  from (4) must be within 1 % of the known  $U_r$ . In the second stage, stratified wave-current boundary layer theory is applied, using  $U_a$  from the first stage as the initial guess for the boundary layer current. The  $U_r$  convergence criterion is reapplied.

The parallel-processing codes developed for this research use two different computational strategies. One-dimensional domain decomposition was used in CH3D-SED and WCBL. A pre-processor divides the grid into a user-specified number of horizontal blocks with approximately equal numbers of water points. A two-dimensional decomposition was not selected since it would have made good load balancing difficult to attain. During the CH3D-SED and WCBL

simulations, the processors for neighboring blocks send each other updated arrays using calls to the Message Passing Interface (MPI) library of functions. A parallel version of WAM was obtained using the OpenMP library. More complete details of the parallelization strategies are contained in Welsh et al. (1999).

### **Inter-model communication**

The CH3D-SED and WAM models must wait while the WCBL model calculates the combined boundary layer parameters. WCBL is, therefore, called as a subroutine by each CH3D-SED process and uses the same domain decomposition as CH3D-SED. Communication between WAM and WCBL uses MPI calls between the WCBL master process and sequential-processing regions of the WAM code. The CH3D-SED and WCBL master processes use MPI to communicate with their slave processes and make the conversions from blocked to domain-wide arrays, and vice-versa, that are a necessary stage of all data exchanges with WAM.

A COMAPS simulation is launched using an “mpirun” command contained in a shell script. The number of WAM threads is set in the shell script using the “MP\_SET\_NUMTHREADS” function. One WAM process and the selected number of CH3D-SED/WCBL processes are specified in the “mpirun” command. The coupled system has been run on the SGI ORIGIN 2000 platform at ERDC MSRC.

### **Inputs to the WCBL model**

The WCBL model requires the following inputs from the other models in the coupled system:

#### WAM

- Near-bottom maximum horizontal excursion due to wave motion,  $A_b$ , and near-bottom maximum wave-induced velocity,  $U_b$ . These quantities can be calculated from the significant wave height using linear wave theory.
- Mean wave direction,  $q_w$ , which is calculated from the wave energy spectrum.

#### CH3D

- The current,  $U_r$ , and current direction,  $q_r$ , at a reference elevation, plus the reference elevation itself,  $z_r$ . The mid-point of the lowest CH3D sigma layer is used for  $z_r$ , and  $U_r$  and  $q_r$  are found using the velocity components calculated at that location.

#### SED

- The user-input specific weight of sediment grains,  $g_s$ , which is generally 2.65.
- The grain size diameter for each user-specified sediment size class,  $D(n)$ .
- The volume-fraction concentration at the reference elevation for each size class,  $C_{vr}(n)$ .
- The fiftieth percentile (by mass) grain size for the active layer of bedload transport,  $D_{50}$ .

## Use of the WCBL results

The results from WCBL are used in the other models in the following manner:

### WAM

- The combined wave-current friction factor,  $f_{cw}$ , is used in WAM in the calculation of the bottom friction energy dissipation rates. The standard WAM algorithm is

$$S_{bf}(\mathbf{w}, \mathbf{q}) = -C_f \frac{k}{\sinh(2kh)} E(\mathbf{w}, \mathbf{q}), \quad (6)$$

where  $C_f$  is a friction coefficient which is set to 0.0077 m/s;  $E(\mathbf{w}, \mathbf{q})$  is the wave energy component in frequency-direction space; wavenumber,  $k$ , is a function of  $\mathbf{w}$  and  $h$ ;  $h$  is water depth; and  $g$  represents gravitational acceleration. Based on Komen et al. (1994; pp. 161-164), the following alternative expression is used in COMAPS:

$$S_{bf}(\mathbf{w}, \mathbf{q}) = -f_{cw} U_{rms}^b \frac{k}{\sinh(2kh)} E(\mathbf{w}, \mathbf{q}), \quad (7)$$

where  $U_{rms}^b$  is the root mean square near-bottom velocity due to the  $E(\mathbf{w}, \mathbf{q})$  component, which can be calculated using linear wave theory.

### CH3D-SED

- The combined wave-current bottom shear velocity,  $U_{*cw}$ , is used to replace the current-induced bottom shear velocity calculated in CH3D-SED from a standard Taylor drag law,  $U_{*c} = \sqrt{C_b} U_r$ , where the bottom drag coefficient,  $C_b$ , is a user-specified constant.

## Adriatic Sea hindcasts

The COMAPS system has been deployed for the Adriatic Sea. A bathymetry grid comprised of 5-minutes longitude by 5-minutes latitude cells was downloaded from the “Data Warehouse” at the Naval Oceanographic Office web site (<http://www.navo.navy.mil/newpage/index4.htm>). The grid was used directly in WAM, and converted to the equivalent Cartesian coordinate grid for use in CH3D-SED. The grid contains 97 computational cells in the longitudinal direction and 73 cells in the latitudinal direction; the CH3D-SED cells vary in size, but are on the order of 7 km (x-direction) by 10 km (y-direction). The WAM deployment uses 25 frequency bins and 24 directional bins. The CH3D-SED vertical grid uses 20 regularly spaced sigma layers. A contour plot of the grid bathymetry is shown in figure 1.

Adriatic Sea hindcasts were performed for the period 2/1/99, 0 UTC to 2/8/99, 0 UTC. Dr. Rich Hodur of the Naval Research Laboratory, Monterey provided wind stress fields for this period.

The fields were calculated by the Mediterranean Sea deployment of the U.S. Navy COAMPS atmospheric circulation model (Hodur, 1993). The hindcast period was selected due to strong wind and wave activity. Throughout the period, wind directions were typically northeasterly and tended to be largest in the northern third of the sea.

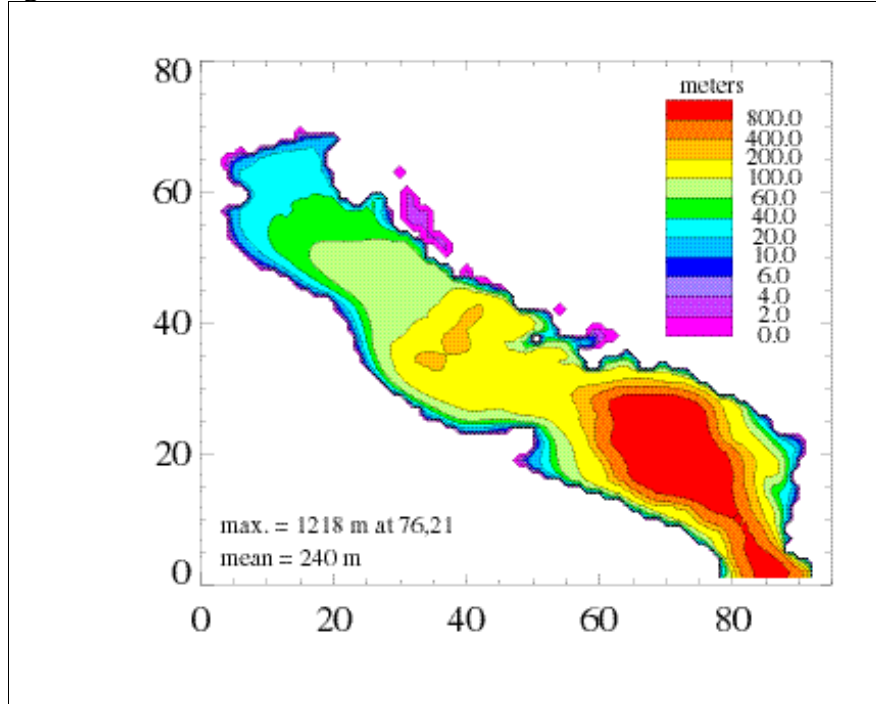


Figure 1: Depth contours and computational cell numbers for the 5-minute Adriatic Sea grid

Quiescent initial conditions were used for WAM waves and CH3D currents. In CH3D, initial temperature and salinity values were set to 4°C and 35 ppm at all grid points. At the open boundary at the southern end of the grid, a diurnal, 1 m tide was imposed. Three sediment size classes were specified in SED, corresponding to typical sand, silt, and clay grains. Initial suspended sediment concentrations were set to zero. The initial (mass fraction) distribution of sediment sizes in the SED active and sub-stratum layers was set to 0.50:0.25:0.25 for the sand, silt, and clay classes, respectively. These are simplistic initial and tidal conditions, but they are sufficiently representative that they do not obscure the impacts of the model couplings in COMAPS. Detailed observational or hindcast data sets were not available for public domain use.

Hindcasts were performed for no model coupling (“0-way”); two-way atmospheric boundary layer coupling only, with WCBL switched off (“2-wayA”); and two-way atmospheric and bottom boundary layer coupling (“2-wayB”). A coupling frequency of 2 minutes was used. Results will be shown for hour-12 of the hindcast period since this time corresponded to the highest storm activity and, therefore, the period of greatest risk for marine operations. The peak wind stress at hour-12 corresponded to a 10-m wind velocity on the order of 30 m/s.

Figure 2 shows contours of the shear velocities calculated in CH3D-SED for hour-12 of the 2-wayB hindcast. In the 2-wayB run, these shear velocities are replaced by the WCBL shear velocities shown in figure 3. It should be noted that values greater than 999. in figures 3 and 6 correspond to the regions where WCBL was unable to converge on a solution. In most cases this

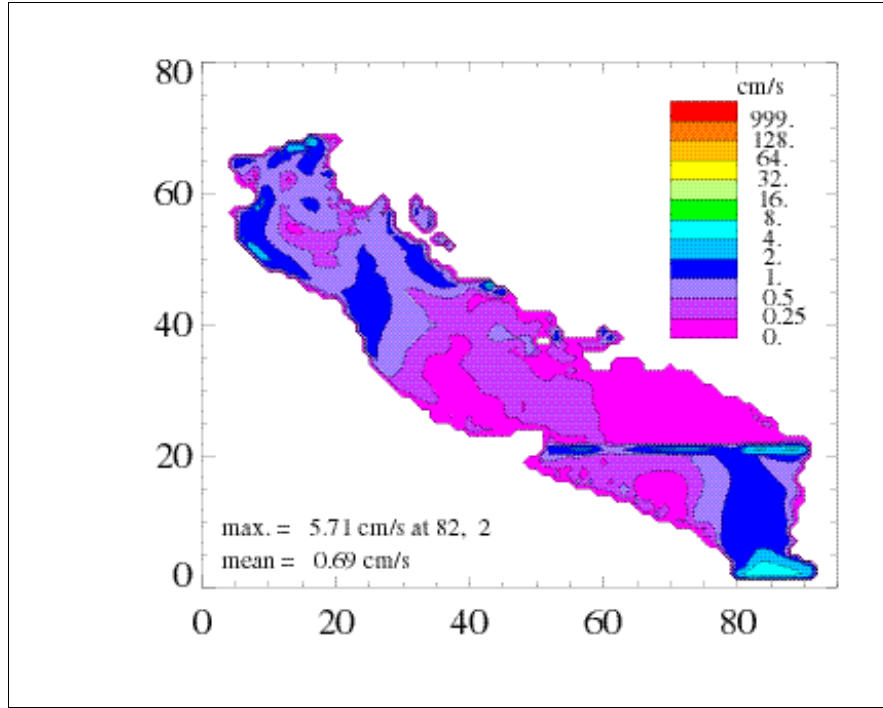


Figure 2: CH3D-SED shear velocities at hour-12 for the two-way coupling (WCBL on) hindcast

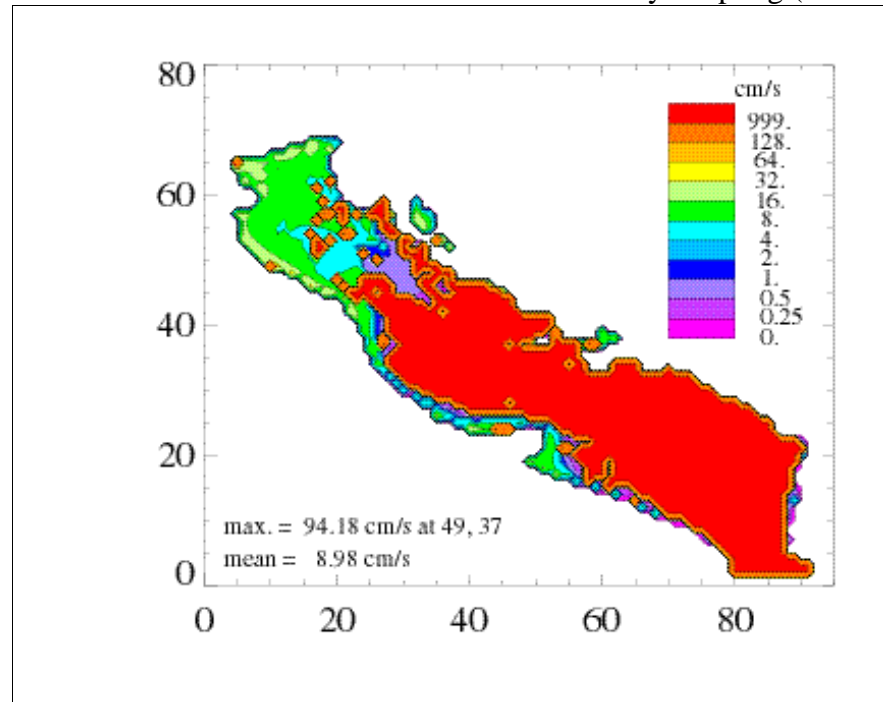


Figure 3: WCBL shear velocities at hour-12 for the two-way coupling (WCBL on) hindcast

occurs when the near-bottom current is much greater than the near-bottom wave-induced velocity, resulting in a violation of model assumptions. This tends to happen in the Adriatic Sea where water depths are greater than 100 m, meaning that wave effects at the bed are negligible and WCBL is not required. WCBL also has convergence problems in very shallow water, as can be seen in Adriatic Sea regions where the depth is less than 4 m. This problem could be related to

the increasing inaccuracy of linear wave theory as depths are reduced. When WCBL cannot converge, the original CH3D-SED shear velocities and WAM friction coefficient are used.

Comparing figures 2 and 3, it can be seen that CH3D-SED and WCBL shear velocities are similar in water depths greater than 60 m (refer to figure 1). This makes sense, as the wave boundary layer will be minimal. As depths fall, however, and wave effects become significant, the WCBL shear velocities become much larger. In water depths less than 20 m, the WCBL shear velocities are generally an order of magnitude greater than the CH3D-SED values. In certain shallow water locations, the ratio of shear velocities reaches two orders of magnitude. This level of increase seems excessive, and is under investigation. Another cause for concern is the band of high shear near the 20<sup>th</sup> row of cells in figure 2. This appears to be related to the border between two blocks in the domain decomposition. This issue is also being investigated.

Figures 4 and 5 shows contours of the clay size class concentration at the lowest sigma layer at hour-12 of the 0-way and 2-wayB hindcasts. The 2-wayA hindcast concentrations are similar to those of the 0-way hindcast. Comparing figures 4 and 5, the enhanced WCBL shear velocities results in larger sediment concentrations, as one would expect. The typical increase is on the order of 200 %. This seems qualitatively reasonable, as large waves in shallow water are likely to generate more sediment transport than the local currents. Excessive increases in concentration are seen in the very shallow regions where shear velocity increases were unreasonably large.

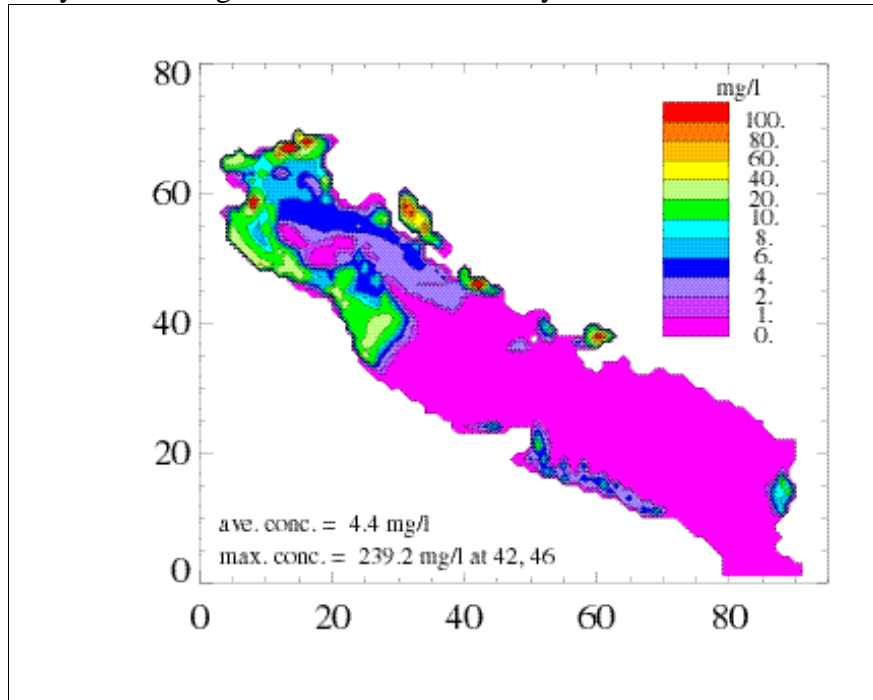


Figure 4: Clay concentrations in the lowest sigma layer at hour-12 of the no-coupling hindcast

Figure 6 shows the hour-12 ratio of the friction coefficient,  $C_f$ , from WCBL to the standard WAM  $C_f$ . Based on equations (6) and (7), the WCBL  $C_f$  is calculated in WAM by multiplying  $f_{cw}$  from WCBL by an energy-weighted  $U_{rms}^b$ . The deep water and very shallow water regions in which WCBL did not converge are again obvious in figure 7. It is interesting to note that the  $C_f$



ratio varies from approximately 0.1 up to 1.6, moving from deep water to very shallow water. This means that the WCBL  $C_f$  varies in a similar fashion, which is qualitatively reasonable since  $U_{rms}^b$  will increase in shallower water and  $f_{cw}$  is likely to increase with  $U_{rms}^b$ . The constant WAM  $C_f$  is in fact unreasonable.

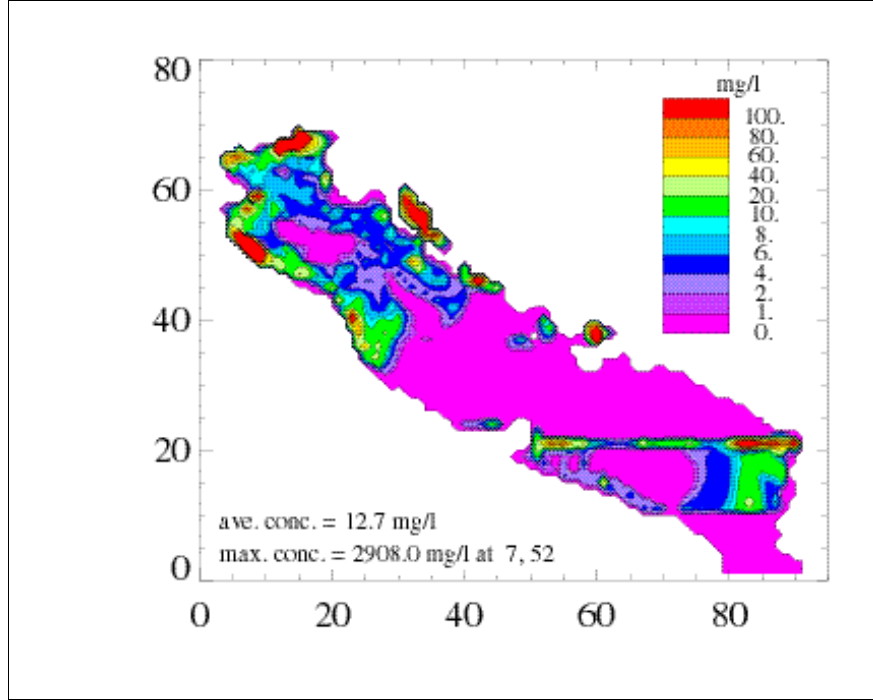


Figure 5: Clay concentrations in the lowest sigma layer at hour-12 of the two-way coupling (WCBL on) hindcast

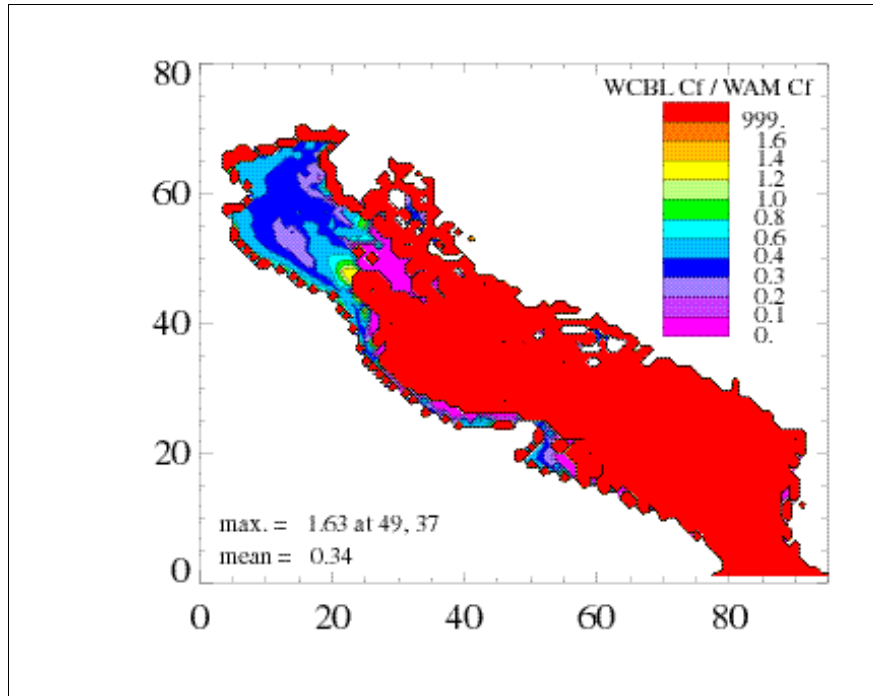


Figure 6: The ratio of WCBL friction coefficient to WAM friction coefficient at hindcast hour-12

Due to space limitations, the effects of WCBL on water elevations and wave height predictions will not be discussed in detail here. Typically, the increased bottom shear velocities reduced CH3D storm surge on the order of 25 %, while the increased bottom friction in WAM reduced shallow water wave heights on the order of 5 %.

## Computational performance results

The coupled system has been run on the SGI ORIGIN 2000 platform at ERDC MSRC. Simulation speed data has been obtained for three sets of runs:

1. number of CH3D-SED/WCBL processes held constant; number of WAM threads varied
2. number of WAM threads held constant; number of CH3D-SED/WCBL processes varied
3. total number of processes held constant, but distribution of processes between CH3D-SED/WCBL and WAM varied to identify the optimal distribution

The latter set of tests most closely represents operational conditions. Figures 7 and 8 show performance results for cases 1 and 3, respectively. It can be seen from figure 7 that the optimum simulation speed for 4 CH3D-SED/WCBL processes is reached with 6 WAM threads. The variation of simulation time with the number of WAM threads shows that CH3D-SED is completing a time step more quickly than WAM. The simulation time rises above 6 WAM threads because the number of computational cells per thread becomes small and communication overhead dominates. For a larger grid, both the rates and limit of performance improvement would be increased. In the coming year, the 5-minute Adriatic Sea grid will be replaced by a 2-minute grid. This will result in improved system scalability and more accurate predictions.

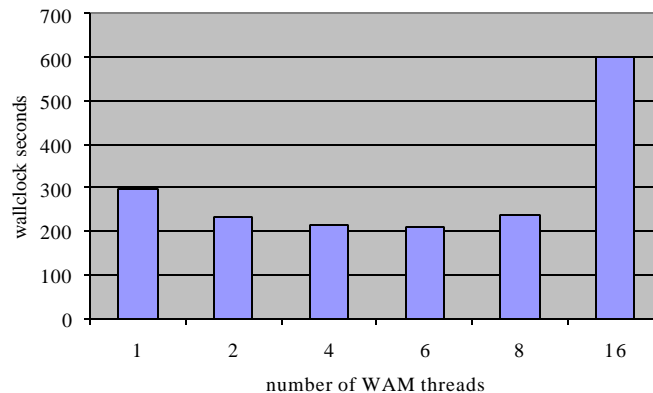


Figure 7: Wallclock time for 1 hr. Adriatic Sea run using 4 CH3D-SED/WCBL processes and a varying number of WAM threads

Figure 8 shows that when 12 processors are to be used, optimum simulation speed is obtained with 8 CH3D-SED/WCBL processes and 4 WAM threads. For this distribution, CH3D-SED and WAM complete a time-step in approximately the same time. It should be noted, however, that two of the runs shown in figure 7 took less time than the fastest run in figure 8. This indicates that it isn't always best to use the total number of processors available if the total number of grid cells is relatively low.

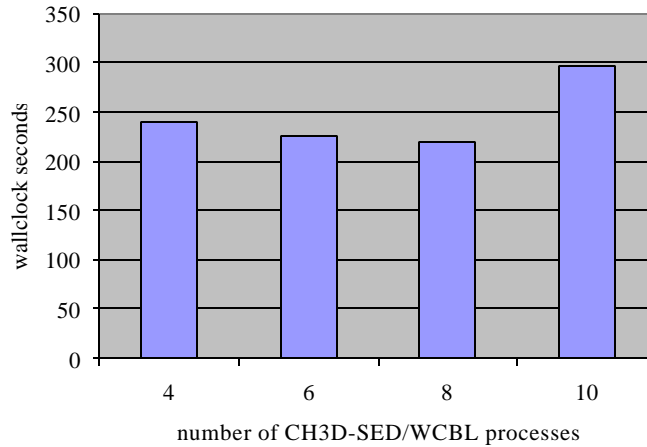


Figure 8: Wallclock time for 1 hr. Adriatic Sea run using a fixed total of 12 processes/threads, but varying the numbers of CH3D-SED/WCBL processes and WAM threads

## Conclusions and future research

Parallel-processing versions of the CH3D-SED marine circulation and sediment transport model, the WAM wind-wave model, and the WCBL bottom boundary layer model have been coupled, resulting in the COupled Marine Prediction System (COMAPS). The system includes couplings at the atmospheric and bottom boundary layers. The integration of WCBL was recently completed. The model simulates the nonlinear interaction of wave and current boundary layers and accounts for stratification due to suspended sediment.

Adriatic Sea hindcasts indicate that WCBL shear velocities are often an order of magnitude greater than the standard CH3D values when large waves are present in water depths less than 20 m. The resulting increases in suspended sediment concentrations can be more than 200 %. While combined shear velocities are likely to become dominated by wave motion in shallow water, the observed levels of increase may be excessive. This issue is under investigation. WAM uses a constant bottom friction coefficient, but WCBL gives coefficients up to 90 % lower in deep water and 60 % higher in very shallow water. This variation is more reasonable. WCBL tends not to converge in water depths greater than 100 m and less than 4 m. This appears to be caused by violations of model assumptions. Where WCBL does not reach a solution, the standard CH3D-SED and WAM bottom boundary layers are used.

COMAPS has been run on the U.S. Army ERDC MSRC ORIGIN 2000 computer and performance measures have been collected for various numbers of processors devoted to the three component models. Results indicate that the number of cells in the 5-minute Adriatic Sea grid is too low for a fair assessment of system scalability. System performance will be tested in the near future using a 2-minute Adriatic Sea grid.

## Acknowledgment

This work was supported in part by a grant of HPC time from the DoD HPC Modernization Program.

## References

- Chapman, R.S., Johnson, B.H. and Vemulakonda, S.R., 1996. User's guide for the sigma stretched version of CH3D-WES; a three-dimensional numerical hydrodynamic and temperature model, *Technical Report HL-96-21*, U.S. Army Engineer Waterways Experiment Station, Vicksburg, MS.
- Glenn, S.M. and Grant, W.D., 1987. A suspended sediment stratification correction for combined wave and current flows, *Journal of Geophysical Research*, **92**: 8244—8264.
- Grant, W.D. and Madsen, O.S., 1979. Combined wave and current interaction with a rough bottom, *Journal of Geophysical Research*, **84**: 1797-1808.
- Gunther, H., Hasselmann, S. and Janssen, P.A.E.M., 1992. The WAM model cycle 4, *Technical Report*, Deutsches KlimaRechenZentrum, Hamburg, Germany.
- Hodur, R.M., 1993. Development and testing of the coupled ocean/atmosphere mesoscale prediction system (COAMPS), *NRL Memorandum Report 7533-93-7213*, Naval Research Laboratory, Monterey, CA.
- Keen, T.R. and Glenn, S.M., 1998. Resuspension and advection of sediment during Hurricane Andrew on the Louisiana continental shelf, *Proceedings of the 5<sup>th</sup> International Conference on Estuarine and Coastal Modeling*, 481-494.
- Komen, G.J., Cavalieri, L., Donelan, M., Hasselmann, K., Hasselmann, S. and Janssen, P.A.E.M., 1994. *Dynamics and Modelling of Ocean Waves*, Cambridge University Press, Cambridge, U.K.
- Lee, J., 1992. An empirical relationship between the bed-load concentration and the excess shear stress in a wave-current boundary layer, *Master's Thesis*, The Ohio State University, Columbus, OH.
- Spasojevic, M. and Holly, M.J., 1994. Three dimensional numerical simulation of mobile-bed hydrodynamics, *Technical Report HL-94-2*, U.S. Army Engineer Waterways Experiment Station, Vicksburg, MS.
- WAMDI, 1988. The WAM model – a third generation ocean wave prediction model, *Journal of Physical Oceanography* **18**: 1775-1810.
- Welsh, D.J.S., Wang, R., Sadayappan, P., and Bedford, K.W., 1999. Coupling of marine circulation and wind-wave models on parallel platforms, *Technical Report ERDC MSRC/PET TR/99-22*, The Ohio State University, Columbus, OH. Prepared for the Department of Defense HPC Modernization Program.